Polish J. of Environ. Stud. Vol. 15 No. 4A (2006), 84-87

Surface Microstructure of Chitosan Membranes – AFM Investigations

Z. Modrzejewska[1], J. Stawczyk[1], K. Matyka[2], M. Matyka[3], I. Mróz[2], A. Ciszewski[2]

[1]Faculty of Process and Environmental Engineering, Technical University of Łódź, ul. Wólczańska 213/215, 93-005 Łódź, Poland
[2]Institute of Experimental Physics, University of Wrocław, Plac Maxa Borna 9, 50-204 Wrocław, Poland
[3]Institute of Theoretical Physics, University of Wrocław, Plac Maxa Borna 9, 50-204 Wrocław, Poland

Abstract

We present the AFM investigations of chitosan membranes' surfaces. We observe the surface microstructures and compare the surface areas of chitosan formate and two forms (white and transparent) of chitosan acetate. The results suggest that the surface of chitosan formate is better developed than the surface of white chitosan aceteate. The transparent chitosan acetate forms the most heterogenous surface.

Keywords*:* chitosan membranes, surface microstructure, AFM

Introduction

Chitosan (Fig.1a) is a natural polymer revealing unique characteristics that predispose it especially to medical applications. Chitosan is biocompatible and biodegradable. It shows athrombogenic and haemostatic properties. One of chitosan's most promising features is its excellent ability to form porous structures [1] that are useful in cell transplantation and tissue regeneration [2]. Many possible medical applications of chitosan-derived materials base on adsorption processes that can occur on the materials' surfaces. Therefore, the surfaces of chitosan-based membranes, films and multilayers are widely discussed (e.g. [3-7]). Their microstructures, including roughness etc. can be effectively investigated using atomic force microscopy (AFM) and related techniques (e.g. lateral force microscopy LFM [7]). In this paper we use the AFM method to investigate the surface microstructure of chitosan acetate and chitosan formate membranes. We compare the surface areas of the membranes and test usefulness of AFM to investigate highly porous materials.

Experimental procedures

Hydrogel chitosan membranes were produced by the wet phase inversion method. Chitosan, low-viscous, of molecular weight 550 kDa and DD=75% (Fluka, 50494) was solved in acetic acid and formic acid to obtain chitosan acetate and chitosan formate as film forming solutions. The amount of acetic acid was 0,42 $g/g_{chitosan}$ and the amount of formic acid was 0,3 $g/g_{chitosan}$. Polymer concentration in the solution was 5% and 7%. The solution was carried out with a mixer (shaker, amplitude of oscillations: 8 mm), at temperature 20^{o}C. After aeration, the solution was poured onto a flat surface (glass plate) using an applicator with a relevant gap (0.9 mm) that resulted in thin films formation. The chitosan membranes were formed by immersing the thin films, immediately after pouring the solution onto a flat surface (before the solvent had evaoporated), into a coagulation bath. The coagulation process was carried out in a 10 % aqueous solution of sodium hydroxide, for 15 minutes. Then the membranes were washed with water and conditioned in demineralized water to obtain pH = 7.0. To preserve their porous structure,

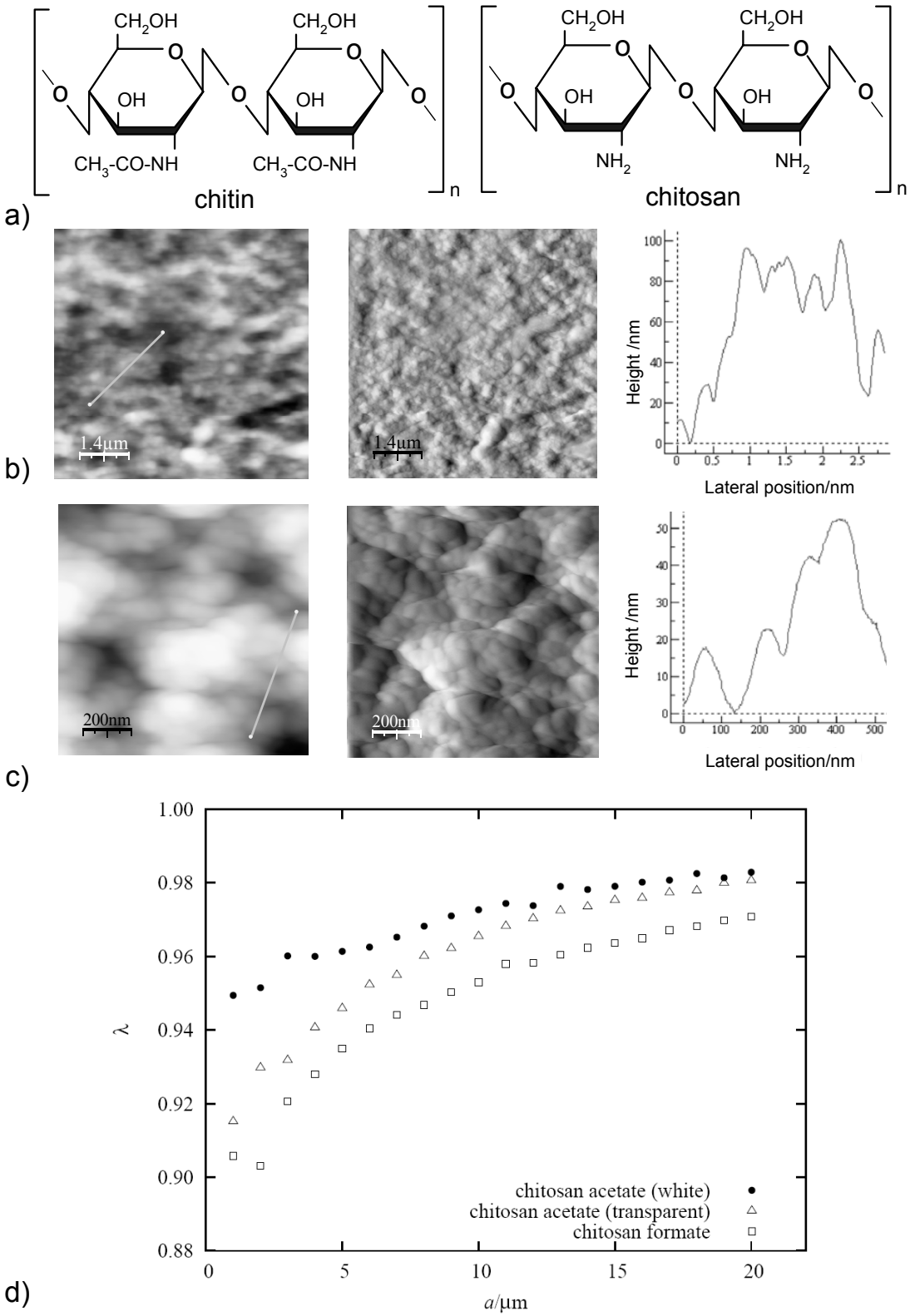

Fig. 1. (a) Chitosan [(1→4)-2 amino-2-deoxy-β-D-glucane] is a product of chitin [(1→4)-2 acetamido-2-deoxy-β-D-glucane] deacetylation. (b) Surface structure of white chitosan acetate, a = 7 μm. The standard Height (left) and Deflection (center) images. The profile (right) is taken along the marked line (c) Higher magnification (a =1 μm) image shows better bulbous structures (left–Height, center–Deflection). (d) An example of the dependence between scan size parameter a and λ. The origin of the observed effects is discussed in the text. For the same scan sizes, smaller values of λ correspond to bigger total surface areas

the membranes in the form of hydrogel were dried by convection at low temperatures, in a closed air cycle. Drying of the membranes was carried out at temperatures –4°C and –12°C, air circulation was 0.6 ms^{-1}. For chitosan acetate we observed two forms of the membranes: transparent (created when the thickness of the hydrogel before drying was about 0.5 mm) and white (thickness about 0.9 mm). The surfaces of the dry membranes were imaged using the Nanoscope IIIa, Veeco, working in the contact mode and equipped with an oxide-sharpened silicon-nitride probe (NP-S). The length and the spring constant of the applied V-shaped cantilever were 196 μm and 0.06 Nm^{-1}, resp. The measurements were performed in air, at room temperature. The lateral and vertical resolutions were 10 nm and 1 nm. The AFM images were processed with the software package WSxM, Nanotec Electronica, Spain [8]. To calculate the total area of an imaged surface we approximated the surface by a triangular mesh using two-dimensional linear interpolation of the standard height map. Then we calculated a sum of the areas of all the triangles constituting the mesh. To compare the surface areas of chitosan acetate (both forms) and formate, we defined a dimensionless parameter λ ($\lambda \leq 1$) as the ratio of the planar area a^2 of an image frame over the total area of the imaged surface, calculated as described above.

Results and discussion

The imaged surfaces show that investigated materials are composed of irregular, bulbous structural elements (Fig.1b,c) of over 100 nm in diameter. The λ parameters were calculated separately for chitosan formate and both forms of chitosan acetate. The results were averaged over 30 independent images for a = 20 μm and the same number of independent images for a = 1μm. For the images of larger area we obtained (mean values λ^{av} and standard uncertainties – experimental standard deviations of the means – $u(\lambda)$): chitosan formate: λ^{av}_f = 0.9744, $u(\lambda_f)$ = 0.0008; chitosan acetate (transparent): λ^{av}_{act} = 0.9771, $u(\lambda_{act})$ = 0.0005; chitosan acetate (white): λ^{av}_{acw} = 0.9808, $u(\lambda_{acw})$ = 0.0005. The corresponding values for the images of smaller area are: λ^{av}_f = 0.8762, $u(\lambda_f)$ = 0.0071; λ^{av}_{act} = 0.864, $u(\lambda_{act})$ = 0.013; λ^{av}_{acw} = 0.9058, $u(\lambda_{acw})$ = 0.0055. The results suggest that the surface of chitosan formate is better developed than the surface of white chitosan acetate. The surface of transparent chitosan acetate should be the most heterogenous since the corresponding $u(\lambda)$ obtained for the images of smaller area is the biggest. For the images of larger area, averaging connected with AFM image formation eliminates the effect of heterogeneity.

The presented numerical values are however influenced by several factors. Firstly, the approximation of the surface by a triangular mesh eliminates structural details and reduces the calculated total surface area. The effect is stronger for the images of larger area. Secondly, the quality of surface imaging depends on the scanning velocity. For rough and extended surfaces, the optimal scanning frequency is about 1 Hz. If the same frequency is applied for scanning of the regions of different areas, the corresponding tip velocity changes. We tested the influence of the scanning rate on the surface corrugation registered on the AFM patterns and we can conclude that the image of the same area (a = 10 μm) obtained using faster scanning looks flatter than those obtained using slower one (the structural details of the surfaces are eliminated if the scanning is too fast). Both factors mentioned above explain the influence of the dimension of the scanned area on λ. The typical relation we observed is presented in Fig. 1 d. The measurements were done for the same scanning frequency, for a = 1,2,…,20 μm. Significant deviations from the presented plots are possible for the smallest scans, especially for transparent chitosan acetate.

Another effect that is usually observed for surfaces of materials composed of spherical/bulbous elements is related to the shape of the used cantilever. In this case the imaged surfaces are “flatten” and their total areas of the surfaces are smaller. Finally, we have some dependence on softness of the material that may be deformed by the tip during the measurement. The reasons listed above indicate that numerical values of λ can be treated as approximate ones. The observed tendencies are however promising and may give us valuable information about structural properties of chitosan membranes.

Conclusions

Basing on the performed AFM investigations we suggest that for three types of chitosan membranes: chitosan acetate (white and transparent) and chitosan formate, the surface area of chitosan formate is bigger than the surface area of white chitosan acetate. The transparent form of chitosan acetate is characterized by the most heterogenous surface.

References

1. Berger J., Reist M., Mayer J.M., Felt O., Gurny R.: Structure and interactions in chitosan hydrogels formed by complexation or aggregation for biomedical applications. Eur. J. Pharm. and Biopharm. **57** (1), 35, **2004**.
2. Lu G., Zhu L., Kong L., Zhang L., Gong Y., Zhao N., Zhang X.: Porous chitosan microcarriers for large scale cultivation of cells for tissue engineering: Fabrication and evaluation. Tsinghua Sci. Technol. **11** (4), 427, **2006**.
3. Nosal W.H., Thompson D.W., Yan L., Sarkar S., Subramanian A., Woollam J.A.: UV–vis–infrared optical and AFM study of spin-cast chitosan films. Colloid Surfaces B **43** (3-4), 131, **2005**.

4. Nosal W.H., Thompson D.W., Yan L., Sarkar S., Subramanian A., Woollam J.A.: Infrared optical properties and AFM of spin-cast chitosan films chemically modified with 1,2 Epoxy-3-phenoxy-propane. Colloid Surfaces B **46** (1), 26, **2005**.
5. Feng Y., Han Z., Peng J., Lu J., Xue B., Li L., Ma H., Wang E.: Fabrication and characterization of multilayer films based on Keggin-type polyoxometalate and chitosan, Mater. Lett. **60** (13-14), 1588, **2006**.
6. Aimoli C.G., Torres M.A. Beppu M.M.: Investigations into the early stages of "in vitro" calcification on chitosan films. Mater. Sci. Eng. C **26** (1), 78, **2006**.
7. Fu J., Ji J., Yuan W., Shen J.: Construction of anti-adhesive and antibacterial multilayer films via layer-by-layer assembly of heparin and chitosan. Biomaterials **26** (33), 6684, **2005**.
8. WSxM free software downloadable at http://www.nanotec.es.